Electronic Supplementary Material (ESI) for Journal of Materials Chemistry A.


# Supp. Info. – Direct 4D Observations of Electrochemically Induced Intergranular Cracking in NMC811 Particles

Huw C. W. Parks,[1,2] Adam M. Boyce,[1,2,3] Aaron Wade,[1,2]
Thomas M. M. Heenan,[1,2] Chun Tan,[1,2]
Emilio Martínez-Pañeda,[4] Paul R. Shearing,[1,2] Dan J.L Brett,[1,2] Rhodri Jervis[1,2,*]

[1]Electrochemical Innovation Lab,
Department of Chemical Engineering, University College London, London, WC1E 7JE
[2]The Faraday Institution,
Quad One, Harwell Science and Innovation Campus, Didcot, OX11 0RA
[3]School of Mechanical and Materials Engineering,
University College Dublin, Dublin, Ireland.
[4]Department of Civil and Environmental Engineering,
Imperial College London, London, SW7 2AZ
*To whom correspondence should be addressed; E-mail: Rhodri.Jervis@ucl.ac.uk

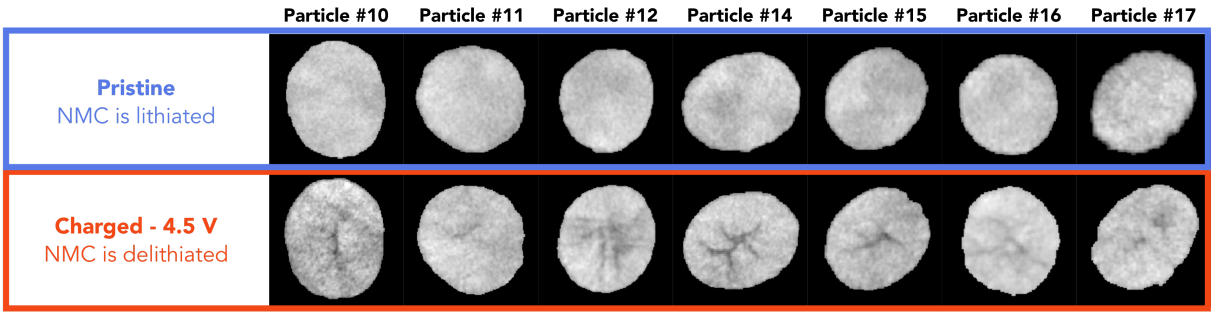


| | | Particle #10 | Particle #11 | Particle #12 | Particle #14 | Particle #15 | Particle #16 | Particle #17 |
|---|---|---|---|---|---|---|---|---|
| **Particle Diameter (µm)** | Pristine | 14.4 | 12.9 | 11.3 | 12.3 | 11.0 | 10.1 | 10.0 |
| | Charged - 4.5 V | 15.3 | 12.8 | 12.3 | 12.9 | 11.4 | 10.7 | 11.0 |
| **Distance From CC (µm)** | Pristine | 28.3 | 22.0 | 44.9 | 31.0 | 33.6 | 40.0 | 8.9 |
| | Charged - 4.5 V | 30.3 | 24.1 | 48.0 | 33.6 | 35.8 | 43.6 | 9.9 |
| **Particle Volume (µm$^3$)** | Pristine | 1563.2 | 1125.6 | 756.0 | 975.0 | 698.1 | 540.1 | 517.0 |
| | Charged - 4.5 V | 1867.4 | 1363.1 | 965.5 | 1130.1 | 785.1 | 634.9 | 700.1 |
| **% Volume Change** | | +16.3 | +17.4 | +21.7 | +13.7 | +11.1 | +14.9 | +26.2 |

Figure S1: Additional particle information from Fig.2

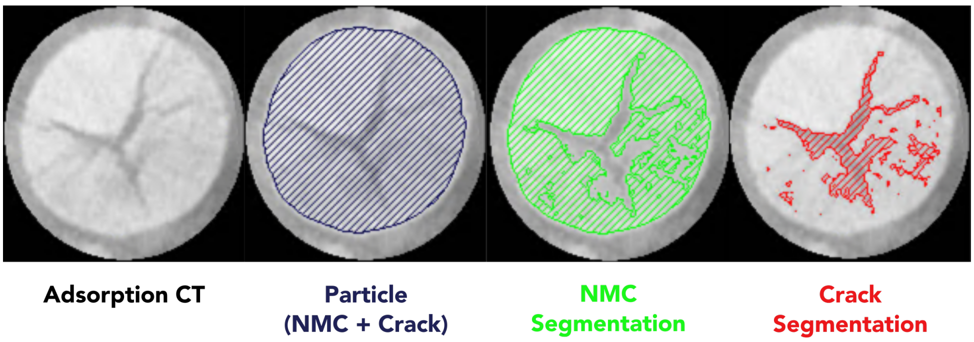


Figure S2: Ortho slices of Particle 3 showing segmentation of different phases used in analysis as shown. Particle analysis was used for particle volume expansion. NMC and crack segmentations were

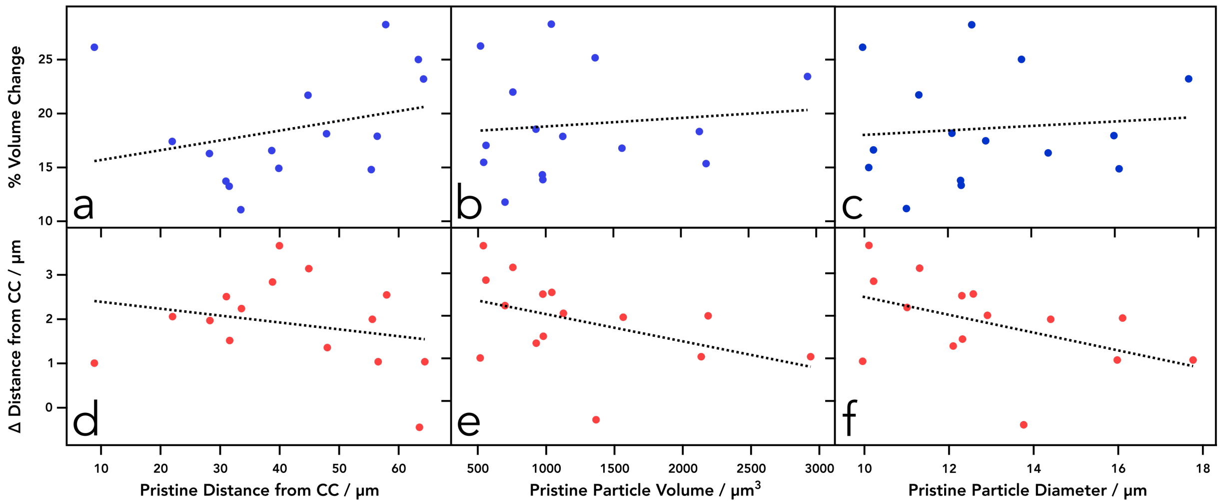


Figure S3: a-c) % Particle volume change upon charging as a function of: a) Distance from current collector, b) Pristine particle volume, c) Pristine particle diameter. d-f) Change in distance of the centre of each particle upon charging with respect to: d) Distance from current collector, e) Pristine particle volume, f) Pristine particle diameter.

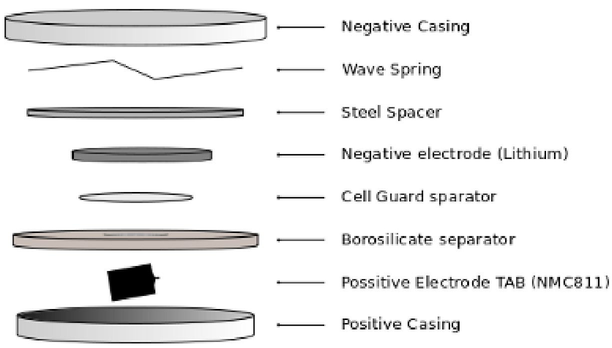


Figure S4: Schematic diagram of coin cell set up for electrochemistry.

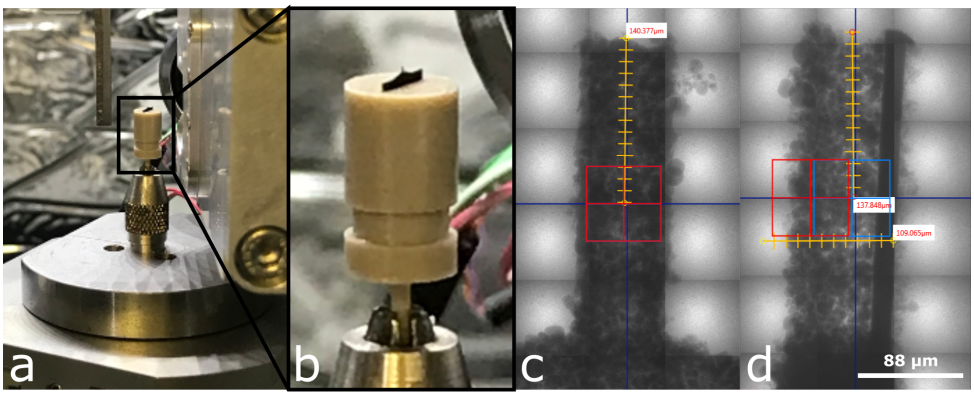


Figure S5: a) Photograph of electrode set up within tomography microscope. b) Zoomed in photograph of the electrode with tab appendage inside custom built holder. c) Radiograph of tab front view with RoI box in red. d) Radiograph of tab side view with RoI boxes in red and blue showing the position at which tomographies were taken.

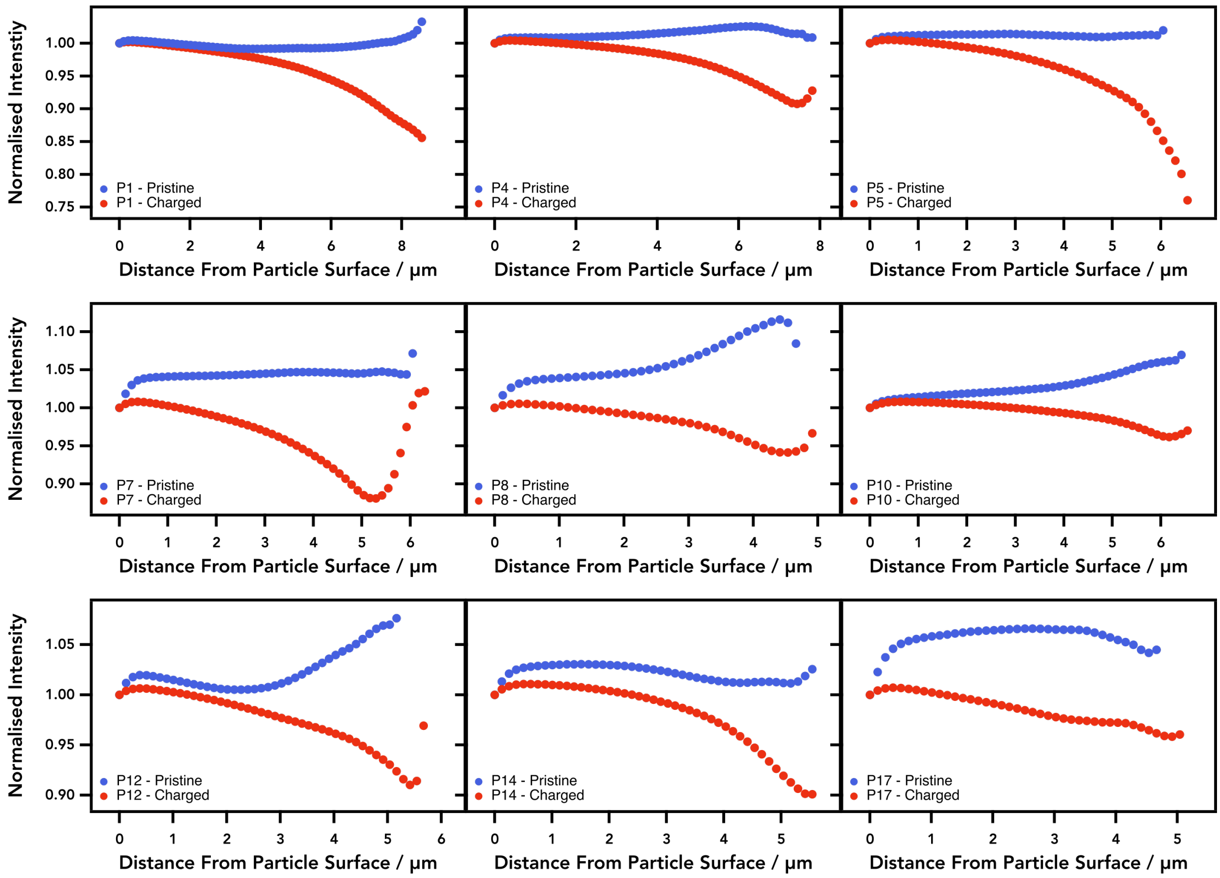


Figure S6: Additional computational analysis using GREAT algorithm to detect the greyscale value of each pixel as a function of distance from the particle surface.

Table 1: Model equations for each domain in the 3D image-based model.

| | Equation | Description | |
|---|---|---|---|
| Single particle transport and electrochemical model | $J_p = -D_p(\nabla c_p + \frac{\Omega c_p}{RT}\nabla\sigma_h)$ | Fick's first law | (1) |
| | $\frac{\partial c_p}{\partial t} + \nabla \cdot J_p = 0$ | Fick's second law | (2) |
| | $i_{app}/i_0 = sinh^{-1}(\frac{\alpha_a F\eta}{RT})$ | Butler-Volmer type equation | (3) |
| | $i_0 = Fk(c(c_{max} - c))^{0.5}$ | Exchange current density | (4) |
| | $\eta = V - U - \frac{\Omega\sigma_H}{F}$ | Overpotential | (5) |
| | $i_{app} = \frac{Fc_{max}C_R V_p}{3600A_p}$ | Applied current | (6) |
| Mechanical model | $\nabla \cdot \sigma = 0$ | Mechanical equilibrium | (7) |
| | $\varepsilon = \frac{1}{2}((\nabla u)^T + \nabla u)$ | Small strain formulation | (8) |
| | $\varepsilon = \varepsilon^e + \varepsilon^{ch}$ | Total strain | (9) |
| | $\varepsilon^{ch} = f(c/c_{max})$ | Lattice strain | (10) |
| Phase field model | $\frac{d\Pi}{dA} = \frac{d\Psi}{dA} + \frac{dW_s}{dA}$ | Griffith equation of fracture | (11) |
| | $G_c(\frac{1}{l}\phi - l\nabla^2\phi) - 2(1-\phi)\psi(\varepsilon^e) = 0$ | Helmholtz-type reformulation of Griffith equation | (12) |
| | $h = (1-\phi)^2$ | Damage function | (13) |
| | $\gamma - l_\gamma^2\nabla^2\gamma = 0$ | Auxiliary equation for diffuse grain boundary interface | (14) |
| | $G_c = hG_g + (1-h)G_b$ | Composite fracture toughness function | (15) |
| | $h = (1-\gamma)^2$ | Auxiliary transition function | (16) |

Table 2: Model parameters.

| Parameter | Unit | Value | Source |
|---|---|---|---|
| $D_p$ | $m^2 s^{-1}$ | $f(c_p/c_{p,max})$ | [1] |
| $c_{p,max}$ | $molm^{-3}$ | 51765 | [2] |
| $c_{p0}$ | $molm^{-3}$ | 51765 | N/A |
| $V_p$ | $m^3$ | $1.515 \times 10^{-15}$ | N/A |
| $\alpha_a$,$\alpha_b$ | 1 | 0.5 | N/A |
| $U$ | $V$ | $f(c_p/c_{p,max})$ | [2] |
| $R$ | $Jmol^{-1}\ K^{-1}$ | 8.314 | N/A |
| $T$ | $K$ | 293 | N/A |
| $E_p$ | $GPa$ | 150 | [3] |
| $G_b$ | $Nm^{-1}$ | 0.023 | [3] |
| $G_g$ | $Nm^{-1}$ | 0.27 | [4] |
| $A_p$ | $m^2$ | $6.48\ \times 10^{-10}$ | N/A |
| $C_R$ | 1 | 1/20 | N/A |
| $l$ | m | 3.6e-8 | N/A |
| $l_\gamma$ | m | 3.6e-8 | N/A |
| $\sigma_c$ | GPa | 0.1 | N/A |

Table 3: Nomenclature.

| Parameter | Description | Parameter | Description |
|---|---|---|---|
| $J_p$ | Lithium flux | $D_p$ | Active material utilisation |
| $i_{app}$ | Applied current density | $\eta$ | Overpotential |
| $V$ | Particle potential | $U$ | Equilibrium potential |
| $c_p$ | Lithium concentration | | Initial lithium concentration |
| $V_p$ | Particle volume | $T$ | Temperature |
| $R$ | Universal gas constant | $k$ | Reaction rate constant |
| $\alpha_a$, $\alpha_c$ | Transfer constants | $F$ | Faraday constant |
| $E_p$ | Young's modulus | $G_b$,$G_g$ | Fracture toughness of boundary and grain |
| $u$ | Displacement | $\sigma$ | Stress |
| $i_{app}$ | Applied current | $\Omega$ | Partial Molar Volume |
| $\sigma_H$ | Hydrostatic stress | $\varepsilon$ | Total strain |
| $\varepsilon^e$ | Elastic strain | $\varepsilon^{ch}$ | Lithiation induced strain |
| $l$ | Phase field length | $\varphi$ | Damage parameter |
| $l_\gamma$ | Transition length scale | $\gamma$ | Auxiliary variable |
| $h$ | Auxiliary transition function | $\Pi$ | Total energy |
| $\Psi$ | Strain energy density | $W_g$ | Work of fracture |
| $A_p$ | Particle surface area | $C_R$ | C-rate |

## References

[1] Noh, H. J., Youn, S., Yoon, C. S., Sun, Y. K. (2013). Comparison of the structural and electrochemical properties of layered Li [NixCoyMnz] O2 (x= 1/3, 0.5, 0.6, 0.7, 0.8 and 0.85) cathode material for lithium-ion batteries. Journal of power sources, 233, 121-130.

[2] Chen, C. H., Planella, F. B., O'regan, K., Gastol, D., Widanage, W. D., Kendrick, E. (2020). Development of experimental techniques for parameterization of multi-scale lithium-ion battery models. Journal of The Electrochemical Society, 167(8), 080534.

[3] Xu, B.-X., Zhao, Y., Stein, P. Phase field modeling of electrochemically induced fracture in Li-ion battery with large deformation and phase segregation. GAMM-Mitteilungen 2016 39, 92–109

[4] Stallard, J. C., Wheatcroft, L., Booth, S. G., Boston, R., Corr, S. A., De Volder, M. F., Inkson, B. J., Fleck, N. A. Mechanical properties of cathode materials for lithium-ion batteries. Joule 2022